Jurnal Teknologi

Full Paper

MICROSTRUCTURE OF NANOSILICA MODIFIED BINDER BY ATOMIC FORCE MICROSCOPY

Mohamad Saifullah Samsudin, Ahmad Kamil Arshad*, Juraidah Ahmad, Khairil Azman Masri

Faculty of Civil Engineering, Universiti Teknologi MARA (UITM), Shah Alam, Selangor, Malaysia

*Corresponding author
ahmadkamil@salam.uitm.edu.my

Article history
Received
2nd December 2015
Received in revised form
13th March 2016
Accepted
31st March 2016

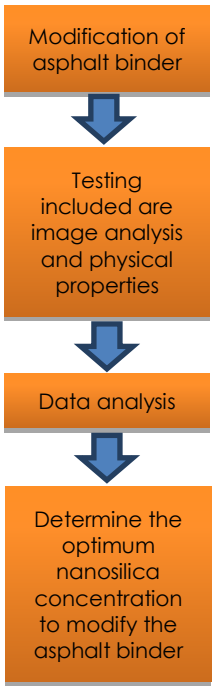

Abstract

In this paper, the effect of nanosilica (NS) on the physical properties as well as aging on the morphology of asphalt binder was investigated. Asphalt binder penetration grade 60/70 (PEN 60/70) was modified with NS at concentrations of 1% to 5% by weight of binder. Scanning electron microscopy (SEM) was used to have a visual evaluation of Nanosilica dispersion. The physical properties tested include is softening point, penetration, ductility, viscosity and storage stability. Temperature susceptibility was evaluated using penetration index (PI) and penetration viscosity number (PVN). Nanosilica modified binder (NSMB) were aged using the rolling thin film oven test (RTFO) and pressure aging vessel (PAV). The morphology of the virgin asphalt binder and NSMB before and after aging was characterized by tapping mode atomic force microscopy (AFM). From the physical properties test, the addition of NS was found to improve the asphalt binder properties and can resist high temperature susceptibility. The results of the AFM imaging showed that the addition of nanosilica in asphalt binder improved its surface stiffness. The overall surface stiffness of the asphalt binder after aging also increased. It can be concluded from this study that 2% to 4% of NS gave the optimum performance for the binder.

Keywords: Nanosilica; atomic force microscopy; scanning electron microscopy; modified binder

1.0 INTRODUCTION

Oxygen and ultraviolet radiation are the main factors of the aging process. Since asphalt binders are composed of organic molecules, it will react with oxygen from the surrounding and change the composition and structure of the asphalt molecules. The term 'age hardening' and 'oxidative hardening' usually refers to the reaction of asphalt and oxygen. The aging of asphalt binder will lead to premature deterioration of the asphalt pavement. At high temperatures, oxidation occurs more quickly compared to low temperature [1]. In the laboratory, the aging of asphalt binder can be accelerated by using rolling thin film oven (RTFO) and pressure aging vessel (PAV). RTFO was used to simulate aging of asphalt binder during storage, mixing, transport and laying down, while PAV was used to simulate the aging during in service life.

The use of nanotechnology in asphalt binder modification promise better results in improving aging resistance. Various materials have been used to modify asphalt binder such as carbon nanotube (CNT) and nanosilica (NS). Santagata *et al.* [2] found that the addition of CNT reduced the susceptibility of asphalt binder to oxidative aging. You *et al.* [3] and

Zafari *et al.* [4] concluded that, NS can be used to improve anti-aging property of asphalt binder.

Previous studies of asphalt have shown that, the scale of observation has decreased from macro scale to micro scale and micro scale to nano scale. Figure 1 shows the multi scale model that has been introduced. The scale consists of; (i) bitumen scale (asphaltene and maltene morphology), (ii) mastic scale (bitumen and filler), (iii) mortar scale (mastic and aggregate where d < 2mm), (iv) asphalt scale (mortar and aggregate where d > 2mm) and (v) continuum scale (road). Continuum scales (road) are often used to predict the overall performance and in-service life of asphalt pavement by laboratory and field test. However, asphalt properties of micro and nano scale always require macroscopic investigation. For example, the rheological properties of asphalt binder, which contribute significantly to the final performance of asphalt pavement, are shown to be related to asphalt structures at the micro and nano scales [5]. There are various microscopy techniques that have been used to evaluate microstructure of asphalt such as scanning electron microscope (SEM), field emission scanning electron microscope (FESEM), and atomic force microscopy (AFM).

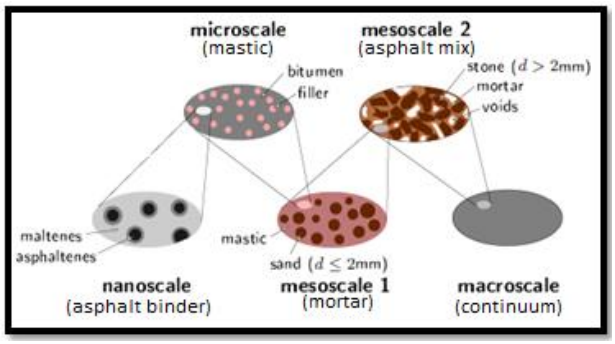

Figure 1 Multi scale model for asphalt [9]

AFM was introduced by Binning *et al.* [6] to measure the surface force and surface topography. Loeber et al. [7, 8] used AFM to observe the topography of asphalt binder. The AFM images of heat-cast asphalt samples revealed the ripple microstructure with tens of nanometer in height and several micrometers in diameter. 'Bumble bees' term was used to name these ripples microstructure which resembled the yellow and black strip. The authors suggested that the composition of these structures was attributed to the asphaltenes. Other shapes and texture, including networks and spherical clusters were also observed in this study.

Jager *et al.* [9] used AFM with non-contact mode (NCM) and pulsed-forced mode (PFM) in their study to investigate five different types of bitumen and phases in bitumen. The image of NCM and PFM showed the same images as previous research, which is 'bee-shaped' structure and matrix phase. Four subdomains were identified from the surface topography such as (i) high part 'bees' (bright area, larger stiffness, lower adhesive) (ii) lower part 'bees' (dark area, lower stiffness, high adhesive) (iii) high part matrix (surrounding 'bees') (iv) lower part matrix (far away from 'bees', low stiffness).

The AFM indentation method was performed by Daurado et al. [10] in order to relate the features observed to its local stiffness and elastic recovery. They found that the overall elastic modulus of the region containing the bees is lower than the one observed in the matrix. The bright area of the bee also presented a lower elastic modulus (~9 N/m) compare to the overall bee area (~12 N/m). These results contradicted with the findings by Jager *et al.*

Lyne *et al.* [11] used AFM quantitative nanomechanical propertiy (QNM) mapping (surface force mapping technique) to evaluate topography, adhesion and elastic modulus of asphalt binder with different refractive index. From the topography image, typically phases are observed. They used catana phase as a term to represent the typical bee structure, peri phase to represent area surrounding catana phase and para phase to represent the area neighbouring to peri phase. The result showed that, the adhesive force in catana and peri phase are lower than the adhesive force in para phase while Young's moduli in the catana and peri phase are higher than the Young's modulus in para phasa. These results are similar to the result obtained by Jager et al.

Finally, various AFM techniques were used by Nazal *et al.* [12] to study the effect of different warm mix asphalt (WMA) additives on the nanostructure and microstructure together with adhesive and cohesive properties of asphalt binder. The result of an AFM image showed that Sasobit additive reduced the width of bee structure and resulted in increasing the relative stiffness of dispersed domains containing the bee structure compared to those with flat area.

In this paper, AFM tapping modes were used to evaluate the effect of different percentages of nanosilica and different aging conditions on the microstructure of asphalt binder. The effects of nanosilica on physical properties of asphalt binder were also examined.

2.0 EXPERIMENTAL

In this section, material and method of asphalt binder testing were described.

2.1 Materials

The base asphalt binder used in this study was penetration grade 60/70 (PEN 60/70). The properties of NS used in this study are shown in Table 1.

Table 1 Properties of nanosilica

Properties	Value
Appearance	Slightly milky transparent to translucent liquid
SiO2 (wt%)	30±1%
Na2O (wt%)	0.5%
pH (20°C)	8.5-10.5
Density (20°C, g/cm3)	1.19-1.22
Particle size (nm)	10-15

2.2 Binder modification

Asphalt binder was blended with 1% to 5% nanosilica (1% increment) by weight of the virgin asphalt binder. The modification of asphalt binder was conducted by mechanical mixer. Asphalt binder was heated up to 160°C until it achieves the processing viscosity. Cylindrical container was filled with about 400g of hot asphalt and placed on a hot plate. The temperature of hot plate was set to 160°C to maintain the viscosity of asphalt binder during mixing. NS was gradually added into the hot asphalt binder while stirring with mechanical steel stirrer. The speed of stirrer set to 2000 rpm. The mixing process was continued for one hour in order to achieve uniform dispersion of NS. The modified binder was put in the oven to remove the bubbles, before preparing the test sample. To ensure the dispersion of nanosilica in asphalt binder, scanning electron microscopy (SEM) was used. The SEM image of asphalt binder was used to understand the surface morphology and microstructural changes of NSMB. To facilitate in referring each sample, they were named using following abbreviations: BASED, NSMB-1%, NSMB-2%, NSMB-3%, NSMB-4% and NSMB-5%.

2.3 Aging procedures

All asphalt binders were aged by rolling thin film oven (RTFO) and pressure aging vessel (PAV). RTFO was used to simulate short term aging and measured the effect of heat and air on a moving film of semi-solid asphaltic binder. A temperature of 163°C for a duration of 85 minute were used to produce aging effects comparable to the average asphalt plant condition. PAV was used to simulate long term aging equivalent to 5-10 years of in-service pavement [13].

2.4 Atomic Force Microscopy (AFM)

AFM was applied to investigate the morphology and microstructure of asphalt binder. In the AFM sample preparation, NSMB was heated up to 160°C and dropped on the glass slide surface. Glass slide was placed in the oven at the same temperature for 10 minutes in order to have a smooth and glossy surface. The samples were cooled at room temperature for 24 hours before being tested. The dimension of asphalt droplet should be around 1 cm in diameter as shown in Figure 2. The sample must be kept in a closed container to prevent the sample surface from any disturbance such as dust. This is because the disturbed sample surface will highly affect the AFM image. In this study, a non-contact AFM (model EX-100) was used. Topographic image was scanned using silicon probe. The cantilever was 125 µm long with curvature radius of 5-10 µm. The drive frequency was about 300 kHz and the scan rate was 0.5 Hz. All AFM images were measured in dimension of 20 µm x 20 µm.

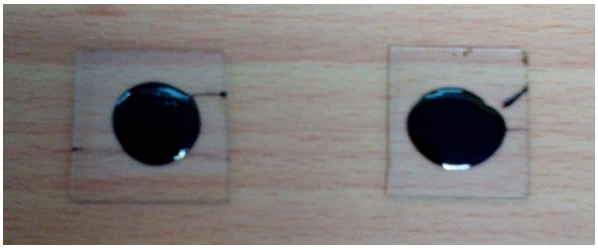

Figure 2 AFM samples

2.5 Phase distribution analysis

Box counting method was used to analyze the phase distribution of AFM image. In this method, a binary image is covered with square of a certain size using the smaller square size.

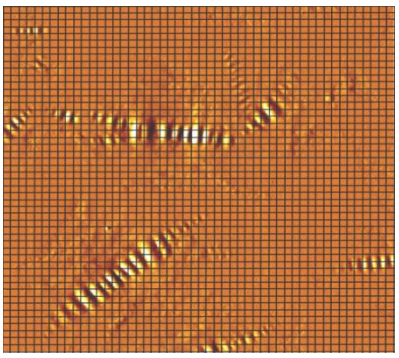

Figure 3 Box counting method (50 x 50)

Phase distributions were analyzed in terms of percentage (%) and are given by the following equation:

$$\text{Phase distribution (\%)} = \frac{number\ of\ box\ to\ cover\ the\ image}{total\ number\ of\ box} \times 100 \quad (1)$$

2.6 Physical Properties Test

The physical properties of NSMB were characterized using conventional methods such as softening point test, penetration test, ductility test, storage stability and viscosity test. The softening point test as to ASTM was D36 used to determine the consistency of

binder. Penetration test as to ASTM D5 was used to evaluate the consistency of an asphalt binder. Ductility test measured the ability of asphalt binder to elongate before breaking. Storage stability was used to evaluate the high temperature storage stability of modified asphalt. Rotational Viscometer test ASTM D 4402 was used to measure viscosity of the asphalt binder at application temperature to determine the handling and pumping properties at the terminal, plant facility and refinery.

2.7 Temperature susceptibility

Penetration index (PI) and penetration viscosity number (PVN) were calculated to determine the changing of temperature susceptibility of NSMB. PI value was determined from result of penetration test at 25°C and softening point (ball and ring) test. PI was determined by using nomograph or using the following equation:

$$PI = \frac{1952 - 500 \log Pen - 20S.P}{50 \log Pen - S.P - 120} \quad (2)$$

where Pen is the penetration value at 25°C and S.P is the softening point value. The PVN was determined from the results of penetration test at 25°C and viscosity test at 135°C using the following equation:

$$PVN = -1.5 \frac{4.258 - 0.7967 \log P - \log V}{0.795 - 0.1858 \log P} \quad (3)$$

where P is a penetration value at 25°C and V is a viscosity value for 135°C.

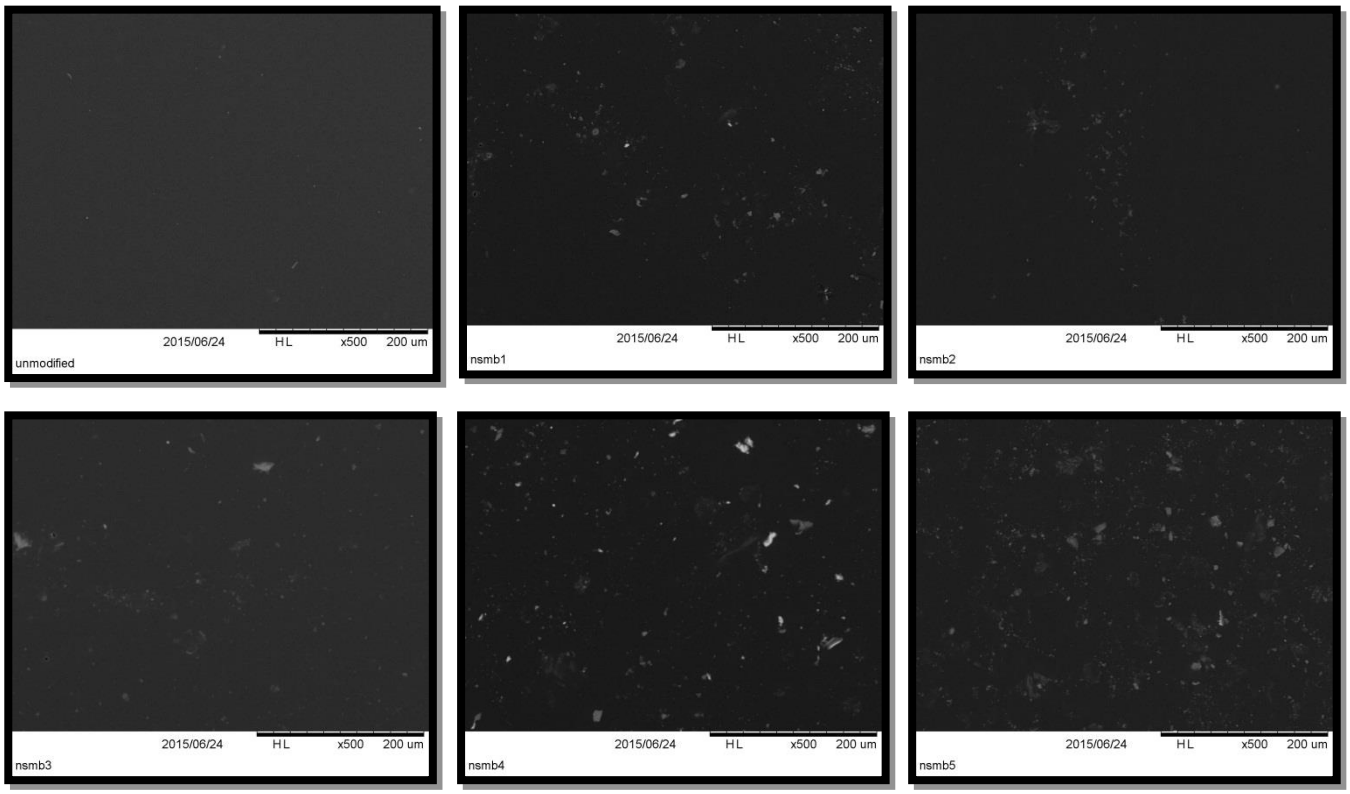

Figure 4 SEM image. From top left 0%, 1%, 2%, 3%, 4% and 5%.

3.0 RESULTS AND DISCUSSION

3.1 Scanning Electron Microscopy image

In order to understand the microstructure changes of the NSMB and the physical dispersion of the nanosilica particles in asphalt binder, Scanning Electron Microscopy (SEM) was used. Figure 4 shows the microstructure of NSMB that was changed significantly compared to the base asphalt binder. The white spots as shown in the SEM image represent nanosilica particles. The SEM image of NSMB shows the well-dispersed nanosilica particles in the asphalt binder matrix. The new structure of asphalt binder was developed. However, nanosilica seemed to agglomerate in asphalt binder where the nanosilica becomes tens or hundreds nanometers in size. Due to the agglomeration of nanosilica, surface area between nanosilica and asphalt binder becomes smaller. Well dispersion of nanosilica in asphalt binder may be helpful for the modulus improvement of nanosilica modified asphalt binder and mixture.

3.2 AFM image

3.2.1 General considerations

Asphalt binder mainly consists of hydrogen and carbon combine (hydrocarbon). Asphalt is composed of four main components; Saturates, Asphaltenes, Resin and Aromatics (SARA). Most asphalt binders contain heteroatoms such as oxygen, nitrogen and sulfur. Besides that, asphalt binder also contains less than 1% of metal such as; nickel, iron and vanadium [14]. Figure 5 shows the image of the AFM trial sample and the phases observed. Three phases are typically observed in the AFM image as found by other researchers (Loeber et al. [7], Jäger et al. [9] and Lyne et al. [11]): (i) Catana phase that represents the typical bee structure (bright and dark line indicates a rise and drop of the topographic line), (ii) peri phase that is peripheral to the catana phase, (iii) para phase that is adjacent to the peri phase. Jager et al. [9] suggested that the formation of bee structure can be attributed to the asphaltenes and resins. Mason et al. [15] found that there is a good correlation between the bee structure and the nickel and vanadium in asphalt binder. Finally, Lyne et al. [11] and Pauli et al. [16] suggested that the bee structure can be attributed to the wax content in the asphalt binder. The image obtained using AFM tapping mode was used to examine the effect of nanosilica and aging condition on the microstructure of asphalt binder. The analysis of AFM image included a visual evaluation of the image, phase distribution presence and surface roughness.

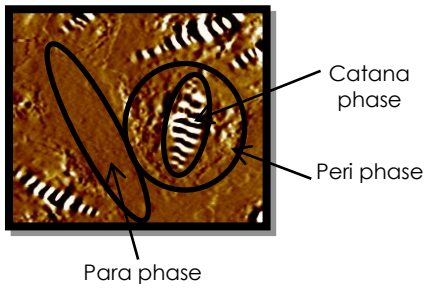

Figure 5 Trial sample and phase distribution

3.2.2 Unaged asphalt binder

Top line in Figure 6 shows the AFM topography image of NSMB for an unaged sample. In this condition, three distinctive phases could be identified in both the control binder and NSMB. NSMB-1% and NSMB-2%, significantly affect the AFM image where the amount of catana phase increased by about 30% and 50% respectively, but for NSMB-3%, NSMB-4% and NSMB-5% samples display nearly the same amount as the control samples. The overall size of catana phase is nearly similar for all samples which are approximately 7 µm – 12 µm in length and 1.0 µm – 1.5 µm in width. The phase contrast between peri and para phase can be seen inverted at higher percentages of nanosilica (NSMB-3% to NSMB-5%) where the para phase increased. Para phase are classified as low stiffness while peri and catana phase classified as high stiffness by Jager et al. [9]. As compared with Jager et al., it can be said that NSMB-3% to NSMB-5% did not have a significant influence to increase the stiffness of NSMB. Table 2 and Table 3 shows that the higher catana phase distribution and value of surface roughness are found at NSMB-2%.

3.2.3 RTFO aged asphalt binder

AFM image of asphalt binder after RTFO aged are shown in the second line of Figure 6. Compared with the unaged sample, the contrast between peri phase and para phase increased remarkably after RTFO aged, where the para phase significantly disappear. Furthermore, the catana phase for NSMB-1%, NSMB-2%, NSMB-3% and NSMB-5% also disappeared. There is only two distinctive phases that could be identified, which is the bright spot and peri phase. This image indicates that the asphalt binder become stiffer after RTFO aged. It can be explained that this is due to bitumen aging, where some chemical reaction occur and molecular structures of bitumen were changed simultaneously. Catana and para phase can only be seen at higher percentages of nanosilica which is NSMB-4% and NSMB-5%. The dimension of catana phase for NSMB-4% and NSMB-5% becomes smaller compared to unaged sample with average length and width approximately 3.5 µm to 4.5 µm and 0.8 µm to 1 µm respectively. In this condition, the highest catana phase was found at NSMB-3%.

3.2.4 PAV aged asphalt binder

Third line of an AFM image in Figure 6 represents the image after aging using the PAV. In this condition, all the three phases could be identified. The size of catana phase for NSMB-0% and NSMB-5% sample was smaller compared to NSMB-1%, NSMB-2%, NSMB-3% and NSMB-4% which are approximately 2 µm – 3 µm in length and 500 nm – 600 nm in width. The other sample dimension is about 7 µm in length and 1.25 µm in width. By comparing with unaged and RTFO aged, PAV aged binder show the highest distribution of catana phase. Again, NSMB-2% shows the highest catana phase distribution and surface roughness. By comparing to the findings by Jager et al [9], Lyne et al [11], and Nazzal et al [12], NSMB-2% can be said as the stiffer sample.

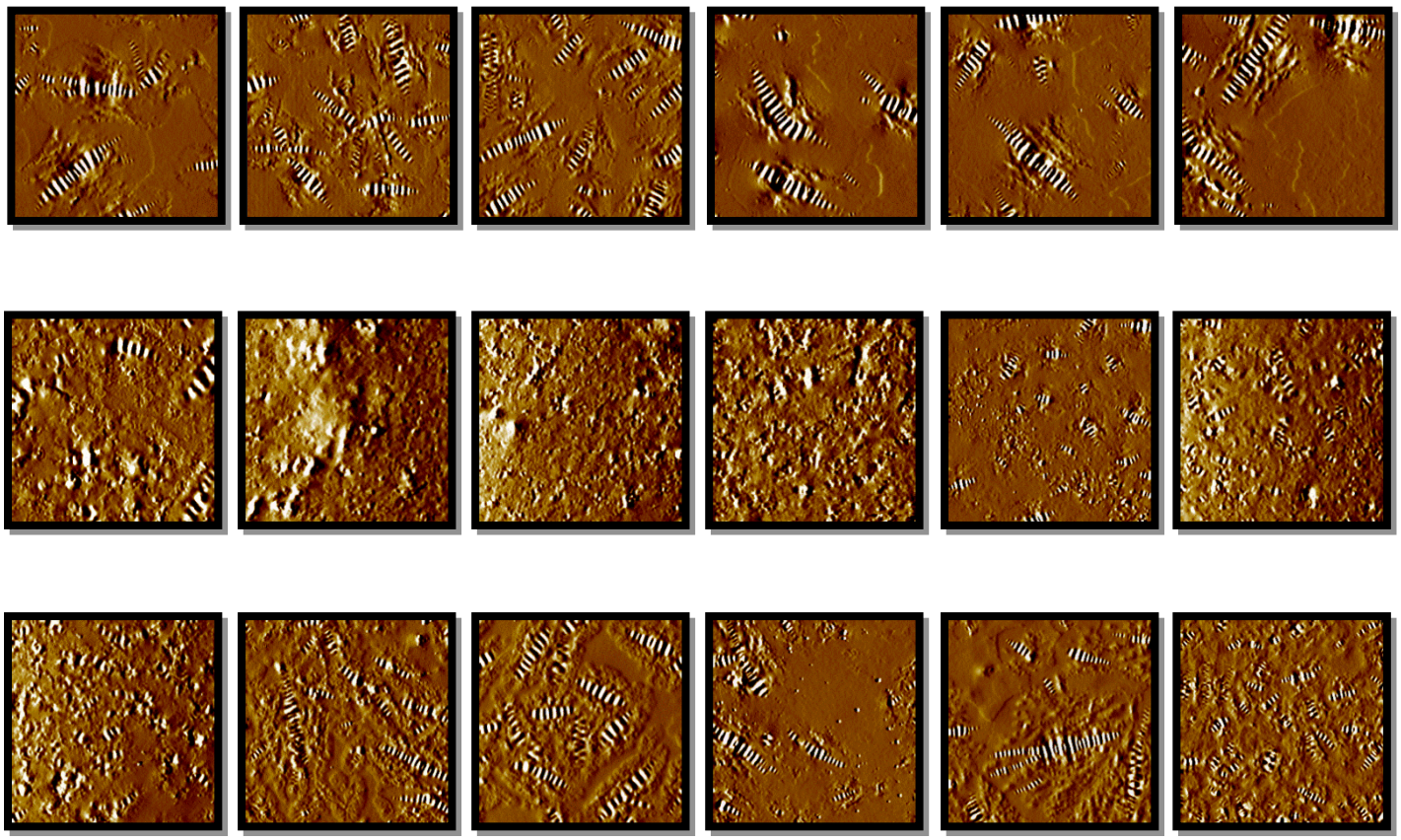

Figure 6 AFM image. From left 0%, 1%, 2%, 3%, 4%, and 5%. Top; unaged sample. Middle; RTFO sample. Bottom; PAV

Table 2 Comparison of phase distribution of asphalt binder

Nanosilica percentage (%)	Phase distribution (%)								
	Unaged			RTFO aged			PAV aged		
	Catana phase	Peri phase	Para phase	Catana phase	Peri phase	Para phase	Catana phase	Peri phase	Para phase
0	10	65	25	12	85	3	14	82	4
1	13	58	29	5	95	NA	21	72	7
2	15	65	20	8	92	NA	22	66	12
3	8	29	63	16	84	NA	13	61	26
4	10	33	57	9	80	11	12	71	17
5	10	40	50	10	90	NA	14	85	1

Table 3 Average surface roughness

Nanosilica percentage (%)	Average surface roughness		
	Unaged	RTFO aged	PAV aged
0	4.191	2.505	0.004
1	4.457	3.204	4.069
2	6.249	3.246	5.062
3	4.342	2.712	2.631
4	5.039	2.152	4.227
5	5.736	0.002	3.164
Average	~5.002	~2.764	~3.831

3.3 Physical properties

Table 4 shows the consistency property value of NSMB with various conventional test methods. Column A shows the penetration value of NSMB for different NS concentrations. Compared to the virgin asphalt binder, NSMB-1% to NSMB-5% show a decrease in the penetration value. This indicates that NSMB is more consistent and harder compared to the virgin asphalt binder. The Softening point value of NSMB is shown in column B. The softening point result shows inverse relation with penetration value, where

NSMB-1% to NSMB-5% show increased in the softening point significantly, compared to the virgin asphalt binder. The highest increasing temperature was obtained at 4% NS which is equal to 11.1°C. The increasing value of softening point indicates that the NS improved the softening temperature of asphalt binder, thus improving its high temperature susceptibility.

Table 4 Consistency properties result

Asphalt binder type	Consistency test					
	A	B	C	D	E	
	Penetration test (dmm)	Softening point test	Ductility test (cm)	Storage stability test	Viscosity test (Pa.s)	
	25°C	(°C)		(°C)	135°C	165°C
BASE	65.0	52.3	140.0	0	0.7	0.3
NSMB-1%	43.5	58.9	129.0	0.2	0.8	0.3
NSMB-2%	41.1	60.3	85.5	0.2	0.9	0.4
NSMB-3%	33.3	62.4	70.2	0.2	1.0	0.4
NSMB-4%	29.1	63.4	51.7	0.3	1.2	0.5
NSMB-5%	30.7	60.0	46.3	0.5	1.2	0.5

Column C shows the ductility value of NSMB. The additions of NS significantly decreased the ductility value of NSMB. A possible explanation for this reduction in ductility is that the dispersion of NS in virgin binder reduces the ability of the virgin binder to elongate.

The storage stability test was used to evaluate the stability and compatibility of the modifier in asphalt binder at high temperature. Since the difference of softening point value between the top and bottom section is less than 2.2°C [19], this means that NSMB is stable when stored at high temperature. Therefore, it can be concluded that NS is a stable material that can be used in asphalt modification.

Column E in Table 4 presents the viscosity value of NSMB at different temperatures. At temperature of 135°C, the viscosity values of NSMB-1% to NSMB-5% increased significantly. Increasing the NS content from NSMB-4% to NSMB-5% does not have significant effect on the viscosity value at 135°C. Similarly, at 165°C, increasing the NS content from 0% to 1%, 2% to 3% and 4% to 5% does not show any significant effect on the viscosity value. The viscosity value of NSMB at 135°C complied with the Superpave standard specification, where the viscosity value for NSMB for all percentages is lower than the maximum limit of 3 Pa. The maximum increase was found with 4% NS for both temperatures, which is 71% for 135°C and 67% for 165°C. The increase in the viscosity value at high temperature is beneficial for rutting resistance.

3.4 Temperature susceptibility

PI and PVN are frequently used to estimate the expected temperature susceptibility for asphalt binder. Table 5 presents the value of PI and PVN of NSMB. According to Read and Whiteoak (17) the value of PI ranges from -3 (highly temperature susceptibility bitumen) to +7 (highly blown low-temperature susceptibility). In this study, the maximum and minimum value of PI is 0.62 and -0.08 respectively. Since all the value of PI is in between +1 and -1, the NSMB is suitable for road construction for all percentages of NS used in this study. According to Briscoe, PVN = 0.0 represents a paving asphalt of low temperature susceptibility, while PVN = -1.5 represents a paving asphalt of high temperature susceptibility [18]. The maximum and minimum values are in range of the value stated. Compared with the PVN value of base asphalt binder, PVN value for NSMB is lower than base asphalt binder. Therefore, these values indicate that all NSMB resist high temperature susceptibility.

Table 5 penetration index and penetration viscosity number

Percentage of nanosilica (%)	Penetration index	Penetration viscosity number
0	0.02	0.103
1	0.47	-0.153
2	0.62	-0.054
3	0.53	-0.131
4	0.43	-0.035
5	-0.08	0.019

4.0 CONCLUSION

The morphology of the NSMB before and after aging was investigated using tapping mode AFM. Most of the AFM images before and after aging displayed the typical bee structure (catana phase). The addition of nanosilica in asphalt binder improved its surface stiffness. The overall surface stiffness of the asphalt binder after aging increased and the surface becomes more solid. Since the AFM tapping mode only displays the microstructure image, the image was compared to previous study to determine the stiffer sample. From the analysis obtained in this study, it can be concluded that NSMB-2% was the stiffer sample for unaged and PAV condition while for RTFO condition NSMB-3% was the stiffer sample. From the physical properties test obtained, 4% of nanosilica shows the optimum performance. NS was also found to resist high temperature susceptibility.

Acknowledgement

The authors expressed utmost gratitude to ZAMALAH grant: 600-RMI/DANA 5/3/PSF (22/2014), Research Management Centre (RMC), University Technology MARA (UiTM) Selangor for financial support.

References

[1] McGennis, R. B., Anderson R. M., Kennedy, T. W., and Solaimanian. M. 1995. Background Of Superpave Asphalt Mixture Design And Analysis. *Federal Highway Administration (FHWA), Report No. FHWA-SA-5-003,* Julai 1995: 1-3

[2] Santagata. E., Baglieri, O., Tsantilis, L. and Dalmazzo, D. 2012. Rheological Characterization Of Bituminous Binder Modified With Carbon Nanotubes. *Social And Behavior Sciences.* 53: 546-555.

[3] Yao. H., You. Z., Li. L., Lee. C. H., Wingard. D., Yap. Y. K., Shi. X., and Goh. S. W. 2013. Rheological Properties and Chemical Bonding of Asphalt Modified With Nanosilica. *Journal of Materials in Civil Engineering.* 25: 1619-1630.

[4] Zafari, F., Rahi, M., Moshtagh, N., and Nazockdast, H. 2014. The Improvement Of Bitumen Properties By Adding Nanosilica.

[5] Lesueur, D. 2009. The Colloidal Structure Of Bitumen; Consequences On The Mechanism Of Bitumen Modification. *Advance In Colloidal And Interface Science.* 145: 42-82.

[6] Binning, G., Quate, C. F., and Gerber. C. 1986. Atomic Force Microscopy. *Phys rev let*. 56(9): 930

[7] Loeber, L., Sutton, O., Morel, J., Valleton, J. M and Muller, G. 1996. New Direct Observations Of Asphalts And Asphalt Binders By Scanning Electron Microscopy And Atomic Force microscopy. *Journal of Microscopy,* 182(1): 32-39. ISSN: 1365-2818.

[8] Loeber, L., Muller, G., Morel, J. and Sutton, O. 1998. Bitumen in Colloidal Science: A Chemical, Structural And Rheological Approach. *Fuel,* 77(13): 1443-1450. ISSN 0016-2361.

[9] Jäger, A., Lackner, R., Eisenmenger-Sittner. C. and Blab, R. 2004. Identification of Four Materials Phases In Bitumen By Atomic Force Microscopy. *Road Materials And Pavement Design.* 5: 9-24. ISSN: 1468-0629.

[10] Daurado, E. R., Simao, R. A., and Leiti. L. F. M. 2012. Mechanical Properties Of Asphalt Binder Evaluated By Atomic Force Microscopy. *Journal Of Microscopy*. 245(2): 119-128.

[11] Lyne, A.L., Wallqvist, V., and Birgisson, B. 2013. Adhesive Surface Characteristics Of Bitumen Binders Investigated By Atomic Force Microscopy. *Fuel* 113: 248-256.

[12] Nazzal, M. D., Qtaish, L. A., Kaya, S., and Powers, D. 2015. Using the Atimic Force Microscopy To Evaluate The Nanostructure And Nanomechanics Of Warm Mix Asphalt. *Journal of Materials In Civil Engineering*. © ASCE, ISSN 0899-1561/04015005(9).

[13] Bahia, H. U., and Anderson, D. A. 1994. *The Pressure Aging Vessel (PAV): A Test to Simulate Rheological Changes Due to Field Aging.* ASTM Special Technical Publication 1241.

[14] Jones, D. R. 1992. *Understanding How the Origin and Composition of Paving-Grade Asphalt Cements Affect Their Performance.* SHRP Asphalt Research Program Technical Memorandum, Strategic Highway Research Program (SHRP) Washington, DC, 4.

[15] Masson, J. F., lebnond, V., and Margeson, J. 2006. Bitumen Morphologies By Phase Detection Atomic Force Microscopy. *Journal Of Microscopy.* 221(1): 17-29.

[16] Pauli, A. T., Grimes, R. W., Beemer, A. G., Turner, T. F., and Branthaver, J. F. 2011. Morphology of Asphalt, Asphalt Fraction And Model Wax-Doped Asphalt Studied By Atomic Force Microscopy. *International Journal Of Pavement Engineering.* 12(4): 291-309. August 2011.

[17] Read, J and Whiteoak, D. 2003. *The shell Bitumen Handbook*. Published for Shell Bitumen by Thomas telford Publishing. Thomas Telford Ltd, 1 Heron Quay, London E14 4JD © Shell UK Oil Products Limited, 2003.

[18] Briscoe, O. E. 1985. *Asphalt Rheologi: Relationship to Mixture : A Symposium Sponsored*. ASTM Committee D-4 on Road and Paving Materials, Nashville, TN, 11 Dec. 1985, Issue

[19] Abdullah, .M. E., Zamhari, K. E., Nayan, N., Hainin, M. R., and Hermadi, M. 2011. Storage Stability And Physical Properties Of Asphalt Modified With Nanoclay And Warm Asphalt Additives. *http://eprints.uthm.edu.my/*